Polymer Chemistry

PAPER

View Article Online
View Journal | View Issue

Cite this: *Polym. Chem.*, 2014, **5**, 3588

"Clicking" fluorinated polyhedral oligomeric silsesquioxane onto polymers: a modular approach toward shape amphiphiles with fluorous molecular clusters†

Bo Ni,[a] Xue-Hui Dong,*[a] Ziran Chen,[a] Zhiwei Lin,[a] Yiwen Li,[a] Mingjun Huang,[a] Qiang Fu,[b] Stephen Z. D. Cheng*[a] and Wen-Bin Zhang*[ac]

Received 1st December 2013
Accepted 8th February 2014

DOI: 10.1039/c3py01670f

www.rsc.org/polymers

Convenient synthesis of fluorinated molecular nanoparticles constitutes a major challenge in the preparation of fluoro shape amphiphiles. To facilitate a modular and efficient synthesis, a "clickable" fluorinated polyhedral oligomeric silsesquioxane functionalized with seven 1*H*,1*H*,2*H*,2*H*-heptadecafluorodecyl side chains and one alkyne group on its periphery (FPOSS-alkyne) was designed and synthesized. It was then used to prepare a series of FPOSS-containing polymers with various architectures *via* "click" chemistry. FPOSS was tethered onto either homo-polystyrene (PS) or polystyrene-*block*-poly(ethylene oxide) (PS-*b*-PEO) at precise locations, including the chain end (FPOSS-PS, FPOSS-PS-*b*-PEO) or junction point [PS-(FPOSS)-PEO], or distributed randomly along a PS chain (PS/FPOSS). This study demonstrates the chemical robustness of the novel building block and establishes a general and efficient approach to introduce fluorous molecular clusters onto polymers, especially for high molecular weight polymers or those polymers with high fluoro contents. These precisely defined FPOSS-containing polymers could serve as model compounds to study the self-assembly behaviors of these shape amphiphiles in the bulk, solution and thin film.

1 Introduction

Fluorous materials have received remarkable attention in a broad range of practical industrial applications including self-cleaning and anti-fouling coatings, non-wetting fabrics, smart surfaces and others, due to their excellent properties.[1–5] In addition to high density, notable thermal stability, and excellent chemical inertness, the most unique property of fluorous materials is omniphobicity, which refers to simultaneous hydrophobicity and oleophobicity, originated from their ultra-low surface energy.[6] The fluorous phase has thus been considered as the "*third*" phase that repels both oil and water.[7] Incorporation of fluorinated components into macromolecules is anticipated to bring novel self-assembly behaviors in the bulk, solution and thin film states, which are not only academically intriguing but also technologically relevant.[8–13] Among them, fluorous molecular clusters are of particular interest.

Fluorinated [60]fullerene (C_{60}) and polyhedral oligomeric silsesquioxanes (POSSs) are two families of fluorous molecular clusters and have attracted much interest, due mainly to their precisely defined nanoscale shape and volume and high fluoro functionalities at the peripheries of these particles.[14–22] Gakh *et al.* reported the first attempt of fluorination of [60]fullerene (C_{60}).[14] The adduct, $C_{60}F_{48}$, however, was found to be unstable in solutions.[14] Recently, Mabry's group developed a series of fluorinated POSS nanoparticles possessing eight fluoroalkyl chains of varying lengths on the vertexes of the POSS cage *via* direct condensation of perfluorinated siloxanes.[16–19] Among them, octakis(1*H*,1*H*,2*H*,2*H*-heptadecafluorodecyl)-POSS was reported to be one of the crystalline solids having the lowest surface energy,[17,19] and was attempted to make superoleophobic surfaces by blending with polymers.[23] Due to high immiscibility between the fluorinated POSS units and the polymer matrix, these blends usually suffer from macro-phase separation that reduces their surface robustness.[18] The poor solubility in common solvents also limits their practical applications.

Covalently incorporating a fluorinated POSS (FPOSS) into polymer chains has been proposed to increase their

[a]*Department of Polymer Science, College of Polymer Science and Polymer Engineering, The University of Akron, Akron, OH 44325-3909, USA. E-mail: scheng@uakron.edu; xd4@zips.uakron.edu; Fax: +1 330 972 8626; Tel: +1 330 972 6931; +1 330 285 2778*

[b]*College of Polymer Science and Engineering, State Key Laboratory of Polymer Materials Engineering, Sichuan University, Chengdu, Sichuan 610065, China*

[c]*Key Laboratory of Polymer Chemistry and Physics of Ministry of Education, College of Chemistry and Molecular Engineering, Center for Soft Matter Science and Engineering, Peking University, Beijing 100871, China. E-mail: wenbin@pku.edu.cn; Fax: + 86 10 6275 1708; Tel: +86 10 6275 2394*

† Electronic supplementary information (ESI) available: The syntheses and detailed experimental procedures. See DOI: 10.1039/c3py01670f

compatibility and processability.[18,24] FPOSS compounds equipped with highly reactive functional groups are thus desired for further derivatization.[18,19] Mabry and coworkers recently reported the synthesis of functionalized FPOSSs possessing alkyl, aryl, or acrylate moieties through a delicate incomplete condensation method.[18] The acrylate functionalized fluorinated POSS was then used as a macro-monomer to copolymerize with methyl methacrylate (MMA) using the reversible addition–fragmentation chain transfer (RAFT) technique.[19] While the work establishes functional FPOSS units including FPOSS-based monomers, a facile and robust route towards FPOSS-containing polymers remains to be highly desired.

Recently, we have demonstrated that "thiol–ene" chemistry is a highly efficient and modular approach[25,26] to prepare functional POSS units and corresponding shape amphiphiles.[24,27–36] A heptavinyl POSS (VPOSS) could be connected to various macromolecules of interest as a precursor *via* either a "grafting-to"[24,27,30–34] or "grafting-from" approach.[24,28,29] The "thiol–ene" reaction between these VPOSS-containing precursors and thiol ligands then quantitatively converts VPOSS into various functional POSS units. For example, facile synthesis of FPOSS-containing polymers has been reported using a combination of ring-opening polymerization (ROP), anionic polymerization, hydrosilylation, and "thiol–ene" reactions.[24] This "post-functionalization" strategy enables the convenient installation of different functionalities onto the same VPOSS-polymer precursors with high efficiency.[30] This method works well using small thiol ligands. However, with bulky ligands, such as the sugar thiols, undesired coupling reactions may compromise this simultaneous multi-site functionalization strategy, which could be occasionally observed as dimers in the SEC chromatograms.[24,28] Similar situations can be observed when fluoroalkyl thiols are involved, especially when the molecular weight of polymers is high and/or when products with high fluoro-content are targeted. To achieve better control, an alternative "pre-functionalization" method is proposed using a "clickable" POSS-based fluorous cluster (FPOSS-alkyne, see below).

In this work, we describe the design and synthesis of FPOSS-alkyne and its utilization in the preparation of FPOSS-containing polymers with diverse topologies using copper catalyzed Huisgen [3 + 2] cycloaddition (CuAAC) "click" chemistry.[37,38] The method is modular, efficient, and robust. By carefully choosing polymer precursors with azido functionalities, a series of FPOSS-containing polymers are prepared where the FPOSS units are precisely located at the chain-end, the junction point, or randomly along a polymer chain of either homo-polystyrene (PS) or polystyrene-*block*-poly(ethylene oxide) (PS-*b*-PEO) (Scheme 1).

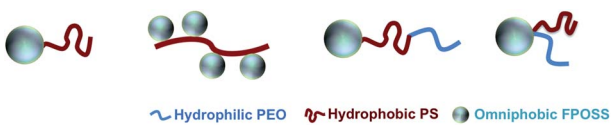

Scheme 1 FPOSS-containing polymers with various architectures.

2 Experimental section

2.1 Chemicals and solvents

The following chemicals were used as received: sodium azide (NaN_3, Aldrich, ReagentPlus®, 99.5%), methanol (MeOH, Fisher Scientific, reagent grade), *N*,*N*-dimethylformamide (DMF, Aldrich, 99.9%), 3,3,4,4,5,5,6,6,7,7,8,8,9,9,10,10,10-heptadecafluorodecane-1-thiol (F8-SH, Aldrich, 98%), *N*,*N*′-diisopropylcarbodiimide (DIPC, Aldrich, 99%), α,α,α-trifluorotoluene (TFT, Aldrich, >99%), 2,2-dimethoxy-2-phenylacetophenone (DMPA, Aldrich, 99%), deuterated chloroform ($CDCl_3$, Aldrich, 99.8 atom % D), and *N*,*N*,*N*′,*N*″,*N*″-pentamethyldiethylene-triamine (PMDETA, Aldrich, 99%). 2,2′-Azobisisobutyronitrile (AIBN, Aldrich, 98%) was purified by recrystallization from ethanol. Cuprous bromide (CuBr, Aldrich, 98%) was purified by stirring in acetic acid overnight, washed with acetone three times, and dried in a vacuum. Chloroform ($CHCl_3$, Fisher Scientific, reagent grade), styrene (Aldrich, 99%), and 4-vinyl benzyl chloride (VBC, Aldrich, >90%) were purified by stirring over calcium hydride for 12 hours and redistilled under vacuum before use. VPOSS-OH and *S*-1-dodecyl-*S*′-(*r*,*r*′-dimethyl-*r*″-acetic acid)trithiocarbonate (TC) were synthesized according to ref. 39 and 40. The carboxylic acid group on TC was further capped with ethanol to give an ester (ETC), as described in the ESI.† Preparation of the azide functionalized polymers, PS-N_3, PEO-*b*-PS-N_3, and PS-(N_3)-PEO, can be found in the literature.[41,42] Synthesis of 4-oxo-4-(prop-2-yn-1-yloxy) butanoic acid is described in the ESI.†

2.2 Instrumentation and characterization

All ^1H and ^{13}C NMR spectra were acquired in $CDCl_3$ using a Varian 500 NMR spectrometer. The ^1H NMR spectra were referenced to the residual proton impurities in the $CDCl_3$ at δ 7.27 ppm. The ^{13}C NMR spectra were referenced to $^{13}CDCl_3$ at δ 77.00 ppm.

Infrared spectra were recorded on an Excalibur Series FT-IR spectrometer (DIGILAB, Randolph, MA) by casting polymer films onto KBr plates from polymer solutions. The data were processed using Win-IR software.

Size-exclusion chromatographic analyses (SEC) were performed using a Waters 150-C Plus instrument equipped with three HR-Styragel columns [100 Å, mixed bed (50/500/103/104 Å), and mixed bed (103/104/106 Å)] and a double detector system with THF as the eluent at a flow rate of 1.0 mL min^{-1} at 30 °C; the detector system consisted of a differential refractometer (Waters 410) and a laser light scattering detector (Wyatt Technology, DAWN EOS, λ = 670 nm). Regular SEC calibrations were conducted with polystyrene standards (Polymer Laboratories).

Matrix-assisted laser desorption ionization time-of-flight (MALDI-TOF) mass spectra were recorded on a Bruker Reflex-III TOF mass spectrometer (Bruker Daltonics, Billerica, MA). The instrument was equipped with an LSI model VSL-337ND pulsed 337 nm nitrogen laser (3 nm pulse width), a single-stage pulsed ion extraction source, and a two-stage gridless reflector.

2.3 Synthetic procedures

FPOSS-OH. VPOSS-OH (200 mg, 0.33 mmol) and DMPA (5.0 mg) were dissolved in a mixed solvent of chloroform and

TFT (1 : 3, v/v). F8-SH (2.06 g, 4.62 mmol) was then added. The solution was irradiated under UV 365 nm for 30 min. After solvent removal, the crude product was purified by flash chromatography on a silica gel column using a mixture of chloroform and hexane (1 : 1, v/v) as the eluent to afford FPOSS-OH as a white powder (0.80 g, 65%). ^{1}H NMR ($CDCl_3$, 500 MHz, ppm, δ): 3.82 (t, 2H, –SiCH$_2$CH_2OH), 2.50–2.85 (m, 28H, –CH_2SCH_2–), 2.20–2.38 (m, 14H, –CH_2CF$_2$–), 1.17 (t, 2H, –SiCH_2CH$_2$OH), 1.06 (t, 14H, –SiCH_2CH$_2$S–). FT-IR (cm^{-1}): 2920, 1532, 1442, 1366, 1331, 1203, 1148, 1111, 1026, 954, 871, 797, 738, 705, 652, 559, 530, 471. MS (MALDI-TOF, Da): calc.: 4032.83, found: 4033.04 $(M\cdot Na)^+$.

FPOSS-alkyne. FPOSS-OH (0.80 g, 0.2 mmol), 4-oxo-4-(prop-2-yn-1-yloxy) butanoic acid (62.4 mg, 0.4 mmol), and DMAP (10 mg, 0.08 mmol) were dissolved in 30 mL of a mixture of dichloromethane and TFT (1 : 3, v/v). DIPC (25 mg, 0.2 mmol) was then added dropwise at 0 °C. The solution was stirred at room temperature for 24 hours. After removal of the solvent, the crude product was purified using a silica gel column. FPOSS-alkyne was obtained by flash chromatography on the silica gel column using a mixture of chloroform and hexane (1 : 1, v/v) as the eluent to afford FPOSS-alkyne as a white powder (0.60 g, 72%). ^{1}H NMR ($CDCl_3$, 500 MHz, ppm, δ): 4.70 (d, 2H, –COOCH_2CCH), 4.20 [t, 2H, –SiCH$_2$CH_2OC(O)–], 2.50–2.85 (m, 28H, –CH_2SCH_2–), 2.60 [t, 4H, –OC(O)CH_2CH_2COO–], 2.45 (t, 1H, –CH$_2$CCH), 2.20–2.38 (m, 14H, –CH_2CF$_2$–), 1.17 (t, 2H, –SiCH_2-CH$_2$O–), 1.06 (t, 14H, –SiCH_2CH$_2$S–). FT-IR (cm^{-1}): 2926, 1738 (C═O), 1648, 1441, 1365, 1331, 1203, 1149, 1113, 955, 868, 795, 737, 705, 652, 557, 530, 472. MS (MALDI-TOF, Da): calc.: 4170.87, found: 4171.39 $(M\cdot Na)^+$.

PS/Cl. ETC (40 mg, 0.10 mmol), styrene (4.0 g), VBC (0.3 g), AIBN (2 mg, 0.01 mmol), and 4 mL of anhydrous toluene were added into a reaction flask equipped with a magnetic stirrer. The flask was degassed by three freeze–vacuum–thaw cycles and immersed into a 110 °C oil bath. After a prescribed time, the flask was quenched by liquid nitrogen. The polymer solution was added dropwise into an excess of cold methanol and the precipitated polymer was collected by filtration. The polymer was obtained after drying *in vacuo* for 24 h (1.8 g, 41.2%). ^{1}H NMR ($CDCl_3$, 500 MHz, ppm, δ): 6.30–7.40 (br, 1200H, aromatic H), 4.52 (br, 20H, –CH_2Cl), 3.30 (br, 2H, CH$_3$CH_2O–), 1.67–2.15 [br, 240H, –CH$_2$CH(–Ar)–], 1.20–1.67 [br, 480H, –CH_2CH(–Ar)–], 0.90–1.10 [m, 31H, –O(C═O)C(CH_3)$_2$CH$_2$–, –S(CH_2)$_{11}$CH_3]. FT-IR (cm^{-1}): 3082, 3059, 3026, 2922, 2875, 1945, 1872, 1790, 1601, 1490, 1453, 1371, 1264, 1176, 1069, 1030, 913, 767, 735, 697, 540. SEC (THF, RI detector): M_n = 23 000 g mol^{-1}, M_w = 23 700 g mol^{-1}, PDI = 1.03.

PS/N$_3$. PS/Cl (M_n = 23 000 g mol^{-1}, N_{cl} = 10; 1.5 g, 0.065 mmol), NaN_3 (81 mg, 1.25 mmol), and anhydrous DMF (5 mL) were added into a round bottom flask with a magnetic stirrer. After stirring for 24 hours, the mixture was diluted with 100 mL of chloroform and washed with water three times. The organic layer was collected and dried under anhydrous Na_2SO_4. After removal of excess solvent, the product was repeatedly precipitated into cold methanol. PS/N$_3$ was obtained after drying *in vacuo* for 24 h (1.2 g, 80%). ^{1}H NMR ($CDCl_3$, 500 MHz, ppm, δ): 6.30–7.40 (br, 1200H, aromatic H), 4.25 (br, 20H, –CH_2N$_3$), 3.30 (br, 2H, CH$_3$CH_2O–), 1.67–2.15 [br, 240H, –CH$_2$CH(–Ar)–], 1.20–1.67 [br, 480H, –CH_2CH(–Ar)–], 0.90–1.10 [m, 31H, –O(C═O)C(CH_3)$_2$CH$_2$–, –S(CH_2)$_{11}$CH_3]. FT-IR (cm^{-1}): 3082, 3060, 3026, 3026, 2883, 2098 (–N$_3$), 1945, 1872, 1800, 1724, 1601, 1493, 1450, 1453, 1369, 1068, 1026, 909, 757, 734, 698, 540. SEC (THF, RI detector): M_n = 16 000 g mol^{-1}, M_w = 18 100 g mol^{-1}, PDI = 1.11.

FPOSS-PS. PS-N$_3$ (M_n = 2400 g mol^{-1}; 55 mg, 0.023 mmol), FPOSS-alkyne (80 mg, 0.02 mmol), CuBr (2 mg, 0.02 mmol), and 15 mL of TFT were added into a Schlenk flask. After three freeze–vacuum–thaw cycles, PMDETA (4 mg, 0.02 mmol) was introduced into the flask under nitrogen protection. After stirring overnight at room temperature, excess PS-N$_3$ was removed with a silica gel column by elution with chloroform. Further elution with a mixture of chloroform and methanol (98 : 2, v/v) gives the product. The solution was concentrated and precipitated into cold methanol three times. The precipitate was collected and dried *in vacuo* for 24 hours to afford FPOSS-PS as a white powder (98 mg, 75%). ^{1}H NMR ($CDCl_3$, 500 MHz, ppm, δ): 6.30–7.40 (br, 120H, phenyl rings), 5.15 [m, 3H, –CH$_2$CH(Ar)N–; triazole–CH_2O–], 4.20 [br, 2H, –(C═O)OCCH_2CH$_2$Si–], 3.40–3.75 [m, 2H, CH$_3$CH_2O(C═O)–], 2.50–2.85 (m, 28H, –CH_2SCH_2–), 2.50 [br, 4H, –OC(O)CH_2CH_2COO–], 2.20–2.38 (m, 14H, –CH_2CF$_2$–), 1.67–2.15 [br, 24H, –CH$_2$CH(–Ar)–], 1.20–1.67 [br, 48H, –CH_2CH(–Ar)–], 0.80–1.20 [m, 25H, –SiCH_2CH$_2$–; CH_3CH$_2$O(C═O)–; O(C═O)C(CH_3)$_2$CH$_2$–]. FT-IR (cm^{-1}): 3082, 3061, 3027, 2926, 2852, 1944, 1872, 1800, 1732 (C═O), 1601, 1493, 1450, 1364, 1238, 1205, 1147, 1028, 955, 871, 754, 699, 652, 532, 465. SEC (THF, RI detector): M_n = 4800 g mol^{-1}, M_w = 5400 g mol^{-1}, PDI = 1.12. MS (MALDI-TOF, Da): calc.: 5868.71, found: 5869.17 $(M_{14}\cdot Ag)^+$.

PS/FPOSS. PS/N$_3$ (M_n = 23 000 g mol^{-1}; 100 mg, 0.004 mmol; n_{azide} = 0.04 mmol), FPOSS-alkyne (180 mg, 0.043 mmol), CuBr (5 mg, 0.035 mmol), and 10 mL of TFT were added into a Schlenk flask. After three freeze–vacuum–thaw cycles, PMDETA (12.0 mg, 0.07 mmol) was introduced into the flask under nitrogen protection. After stirring overnight at room temperature, excess FPOSS-alkyne was removed with a silica gel column by elution with chloroform. Further elution with a mixture of chloroform and methanol (95 : 5, v/v) gives the product. The solution was concentrated and precipitated into cold methanol three times. The product was obtained as a white powder (200 mg, 71.4%). ^{1}H NMR ($CDCl_3$, 500 MHz, ppm, δ): 6.30–7.40 (br, 1200H, aromatic H), 5.28 (br, 20H, –CH_2–triazole–), 5.15 (br, 20H, –triazole–CH_2O–), 4.15 [br, 20H, –(C═O)OCCH_2CH$_2$Si–], 2.50–2.85 (m, 280H, –CH_2SCH_2–), 2.50 [br, 40H, –OC(O)CH_2CH_2COO–], 2.20–2.38 (m, 140H, –CH_2CF$_2$–), 1.67–2.15 [br, 240H, –CH$_2$CH(–Ar)–], 1.20–1.67 [br, 480H, –CH_2CH(–Ar)–], 0.90–1.10 [m, 31H, –O(C═O)C(CH_3)$_2$CH$_2$–, –S(CH_2)$_{11}$CH_3]. FT-IR (cm^{-1}): 3082, 3061, 3026, 2925, 2853, 1944, 1884, 1807, 1736 (C═O), 1602, 1493, 1450, 1364, 1238, 1206, 1748, 1029, 956, 754, 699, 653, 558, 532. SEC (THF, RI detector): M_n = 79 000 g mol^{-1}, M_w = 89 000 g mol^{-1}, PDI = 1.12.

FPOSS-PS-*b*-PEO. PEO-*b*-PS-N$_3$ (M_n^{PS} = 2800 g mol^{-1}, M_n^{PEO} = 2000 g mol^{-1}; 100 mg, 0.02 mmol), FPOSS-alkyne (102 mg, 0.024 mmol), CuBr (3 mg, 0.024 mmol), and 15 mL of TFT were added into a Schlenk flask. After three freeze–vacuum–thaw cycles, PMDETA (4 mg, 0.024 mmol) was introduced into the flask

under nitrogen protection. After stirring overnight at room temperature, excess FPOSS-alkyne was removed by eluting from the silica gel column with chloroform. Further elution with a mixture of chloroform and methanol (95 : 5, v/v) gives the product. The solution was concentrated and the product was precipitated into cold hexanes three times. The product was collected as a white powder by filtration (142 mg, 71% yield). ^{1}H NMR ($CDCl_3$, 500 MHz, ppm, δ): 6.30–7.40 (br, 140H, aromatic H), 5.15 [m, 3H, –C*H*(–Ar)N–; triazole–CH_2O–], 4.20 [br, 2H, –(C═O)OCCH_2CH$_2$Si–], 3.50–3.80 (m, 180H, –CH_2CH_2O–), 3.40 (s, 3H, CH_3O–), 2.50–2.85 (m, 28H, –CH_2SCH_2–), 2.50 [br, 4H, –OC(O)CH_2CH_2COO–], 2.20–2.40 (m, 14H, –CH_2CF$_2$–), 1.70–2.20 [br, 28H, –CH$_2$C*H*(–Ar)–], 1.20–1.67 (br, 56H, –CH_2CH(–Ar)–), 0.80–1.20 [m, 25H, –SiCH_2CH$_2$–; CH_3CH$_2$O(C═O)–; O(C═O)C(CH_3)$_2$CH$_2$–]. FT-IR (cm^{-1}): 3082, 3060, 3026, 2920, 2872, 1944, 1884, 1807, 1733 (C═O), 1601, 1491, 1450, 1351, 1242, 1205, 1114, 1053, 1029, 953, 758, 700, 660, 531. SEC (THF, RI detector): M_n = 11 000 g mol^{-1}, M_w = 12 300 g mol^{-1}, PDI = 1.11.

PS-(FPOSS)-PEO. The "click" reaction was carried out using a similar procedure to that of FPOSS-PS-*b*-PEO to afford PS-(FPOSS)-PEO in 75% yield from PS-(N$_3$)-PEO (M_n^{PS} = 5200 g mol^{-1}, M_n^{PEO} = 2000 g mol^{-1}) to afford PS-(FPOSS)-PEO. ^{1}H NMR ($CDCl_3$, 500 MHz, ppm, δ): 7.50 (1H, br, triazole), 6.30–7.40 (br, 260H, aromatic H), 5.20 (s, 2H, triazole–CH_2 O–), 4.6–4.7 [1H, br, –C*H*(–Ar)Br], 4.18–4.4 [br, 3H, –(C═O)OCCH_2CH$_2$Si–; –OCH$_2$C*H*(CH$_2$N–)O–], 3.50–3.80 (m, 180H, –CH_2CH_2 O–), 3.40 (s, 3H, CH_3O–), 3.00–3.20 (2H, br, –CH_2N–), 2.50–2.85 (m, 28H, –CH_2SCH_2–), 2.50 [br, 4H, –OC(O)CH_2CH_2COO–], 2.20–2.40 (m, 14H, –CH_2CF$_2$–), 1.70–2.20 [br, 52H, –CH$_2$C*H*(–Ar)–], 1.20–1.67 (br, 104H, –CH_2CH(–Ar)–], 0.80–1.20 [m, 25H, –SiCH_2CH$_2$–; CH_3CH$_2$O(C═O)–; O(C═O)C(CH_3)$_2$CH$_2$–]. FT-IR (cm^{-1}): 3082, 3060, 3026, 2923, 2871, 1945, 1884, 1807, 1734 (C═O), 1601, 1491, 1450, 1352, 1284, 1242, 1206, 1146, 1115, 1029, 953, 758, 700, 652, 536, 463. SEC (THF, RI detector): M_n = 14 000 g mol^{-1}, M_w = 15 200 g mol^{-1}, PDI = 1.08.

3 Results and discussion

3.1 FPOSS-alkyne as a "clickable" fluorous molecular cluster

In order to take advantage of the CuAAC "click" reaction, FPOSS with an azide or alkyne functionality is desired. Considering that polymers with the azide group can be readily prepared by a combination of controlled/living radical polymerization and nucleophilic substitution with sodium azide,[41,43,44] an alkyne-functionalized FPOSS with long fluoroalkyl side chains could be a model building block to construct FPOSS-containing polymers with various architectures (Scheme 1). The "thiol–ene" reaction provides an efficient approach to install different functional groups onto VPOSS-OH precursors.[25–30,32–34] Long fluoroalkyl thiol ligands, however, usually suffer from their poor solubility in common solvents and thus, a complete installation of fluoroalkyl chains on VPOSS is difficult since the resulting partially fluorinated POSS units tend to precipitate out of the solution during the reaction. A fluorous solvent, α,α,α-trifluorotoluene (TFT), was then used to enhance their solubility. The synthetic route towards FPOSS-alkyne is illustrated in Scheme 2. VPOSS-OH was first coupled with fluoroalkyl thiol ligands, F8-SH, to generate FPOSS bearing seven heptadecafluorodecyl side chains and one hydroxyl group (FPOSS-OH). Further esterification with 4-oxo-4-(prop-2-yn-1-yloxy) butanoic acid afforded FPOSS-alkyne with reasonable yield (72%). A long linkage between the alkyne and the FPOSS cage was designed to increase the reactivity of the terminal functional group, since the alkyne group may be buried inside the bulky fluoroalkyl chains and have limited accessibility.

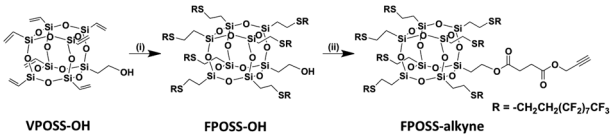

Scheme 2 Synthetic route toward alkyne functionalized fluorinated POSS (FPOSS-alkyne): (i) F8-SH, DMPA, $CHCl_3$: TFT = 1 : 3, UV 365 nm irradiation, 30 minutes, r.t., 65%; (ii) 4-oxo-4-(prop-2-yn-1-yloxy) butanoic acid, DMAP, DIPC, CH_2Cl_2 : TFT = 1 : 3, r.t., 72%.

^{1}H NMR spectroscopy was utilized to monitor the progress of the "thiol–ene" reaction between VPOSS-OH and F8-SH, and the reaction was found to complete within 30 minutes. No precipitation was observed during the irradiation. After the "thiol–ene" reaction, ^{1}H NMR spectra in Fig. 1b show that the resonance peaks corresponding to the vinyl groups on VPOSS-OH at δ 6.00 ppm disappear completely, indicating that all the vinyl groups have been coupled with the F8 chains. New resonances appear at δ 2.5–2.8 and 2.2–2.4 ppm, and can be assigned to the protons on the methylene group adjacent to the sulfur (protons d and e) and to the –CF$_2$– (proton f), respectively. The integration ratio among the peaks of a, d + e, and f is 2 : 29 : 15, close to the proposed structure (2 : 28 : 14), confirming the quantitative functionalization. The MALDI-TOF mass spectrum shown in Fig. 2a also confirms the identity and purity of the

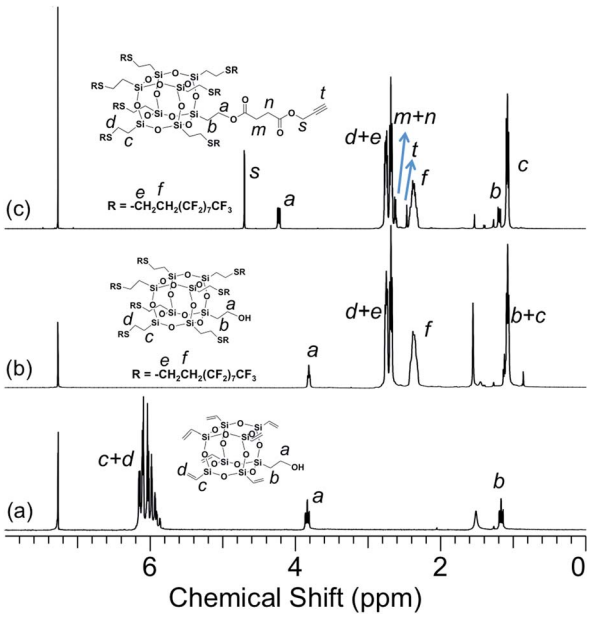

Fig. 1 ^{1}H NMR spectra of VPOSS-OH (a), FPOSS-OH (b), and FPOSS-alkyne (c).

product. A single peak with a molecular weight of 4033.04 Da is found. This is in good accordance with the calculated molecular weight, 4032.83 Da ($[C_{86}H_{61}F_{119}O_{13}S_7Si_8Na]^+$).

Further esterification with 4-oxo-4-(prop-2-yn-1-yloxy) butanoic acid attaches an alkyne functionality on the FPOSS. To obtain a homogeneous mixture, a mixed solvent of TFT and anhydrous CH_2Cl_2 is chosen. The ^{1}H NMR spectrum shows that the resonance at δ 3.8 ppm corresponding to protons on the methylene group adjacent to the hydroxyl group (proton a) shifts completely to δ 4.2 ppm after the formation of the ester group, confirming a quantitative installation of alkyne functionality onto the FPOSS. The resonance of proton on the alkyne (proton t) can be identified at δ 2.4 ppm, while protons on the methylene group adjacent to the alkyne (proton s) at δ 4.7 ppm. The MALDI-TOF mass spectrum provides unambiguous evidence of the success of the esterification. The observed molecular weight is 4171.39 Da while the calculated molecular weight is 4170.87 Da ($[C_{93}H_{67}F_{119}O_{16}S_7Si_8Na]^+$), revealing the preciseness of the product (Fig. 2b).

3.2 "Clicking" FPOSS onto polystyrene: a model reaction

Copper catalyzed Huisgen [3 + 2] cycloaddition (CuAAC) has been widely applied to synthesize polymers with a variety of architectures under mild conditions.[37,38] The high efficiency of "click" chemistry guarantees a quantitative reaction even though the chain-end reactivity of polymers (such as azides) is usually reduced.[41] We take "clicking" FPOSS-alkyne onto PS-N_3 as a model reaction to testify the chemical feasibility and technical simplicity of our strategy. Complicated purification procedures such as fractionation can be avoided. A simple flash chromatography technique will be good enough to remove the catalyst and obtain final products. Azide functionalized PS (PS-N_3) with various molecular weights are prepared using atomic transfer radical polymerization (ATRP) followed by nucleophilic substitution with sodium azide.[41] The synthetic route toward FPOSS-PS conjugates is shown in Scheme 3.

A fluorous solvent TFT is used to increase the solubility of FPOSS-alkyne. A slight excess of PS-N_3 was added to fully consume FPOSS-alkyne. After purification with the silica column, the product shows no trace of the azide adsorption peak (~2100 cm^{-1}) in the FT-IR spectrum (Fig. S1 in the ESI†). In the ^{1}H NMR spectrum, both the resonance peaks representing FPOSS and PS moieties can be clearly identified (Fig. 3). Specifically, the resonances at δ 2.3–2.5 and 2.6–2.8 ppm correspond to the fluoroalkyl chains on FPOSS (protons n, r, and s), while the resonances between δ 6.3–7.0 ppm can be assigned to the aromatic protons on PS (proton f). The covalent connection is also confirmed by the emergence of the resonances at δ 5.2 ppm, which are attributed to the protons adjacent to the newly formed triazole ring (protons g and v). A narrow molecular weight distribution of the FPOSS-PS compound can be identified by SEC. Its retention volume is shifted to a lower value as compared to its precursor, PS-N_3 (Fig. 4).

The MALDI-TOF mass spectrum provides further evidence to prove the success of this model reaction. A single narrow distribution with molecular weights in accordance with the proposed structure is observed (Fig. 5). A representative mono-isotopic peak with m/z = 5869.17 Da is very close to the calculated molecular mass for a 14-mer (5868.71 Da,

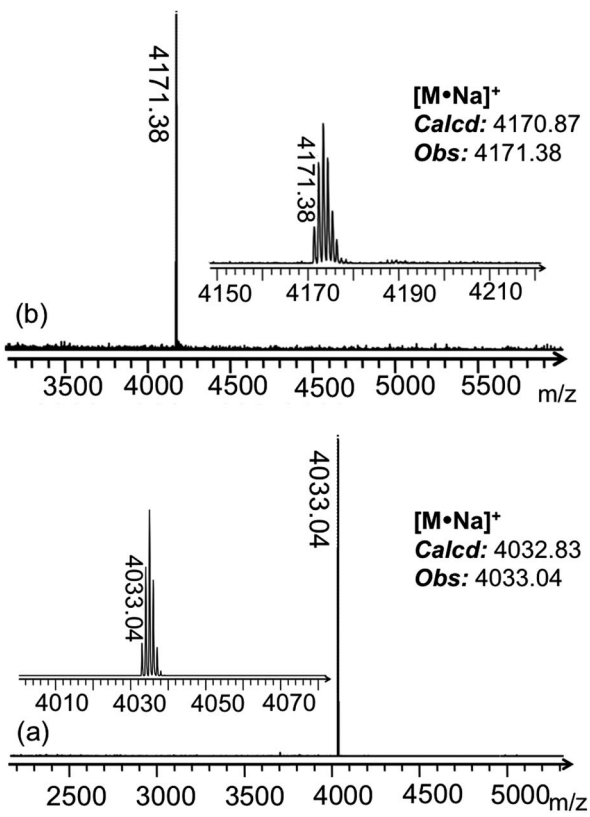

Fig. 2 MALDI-TOF mass spectra of FPOSS-OH (a) and FPOSS-alkyne (b).

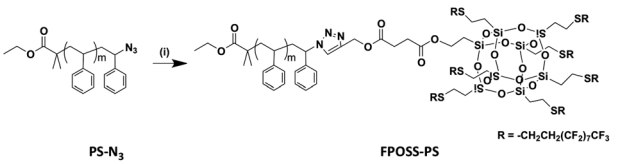

Scheme 3 Synthetic route towards FPOSS-PS: (i) CuBr, PMDETA, TFT, r.t., 72%.

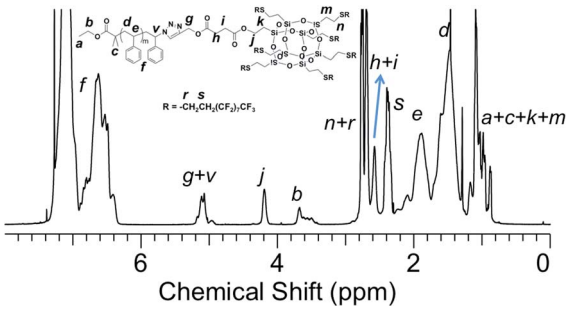

Fig. 3 ^{1}H NMR spectra of FPOSS-PS. The results are based on the sample FPOSS-PS_{24}.

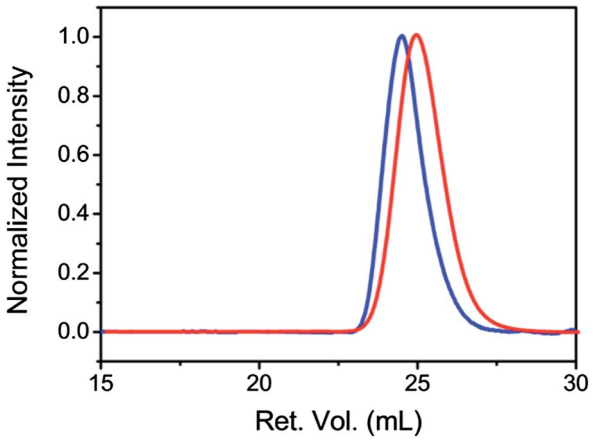

Fig. 4 SEC chromatograms of PS-N_3 (red) and FPOSS-PS (blue). The results are based on the sample FPOSS-PS_{24}.

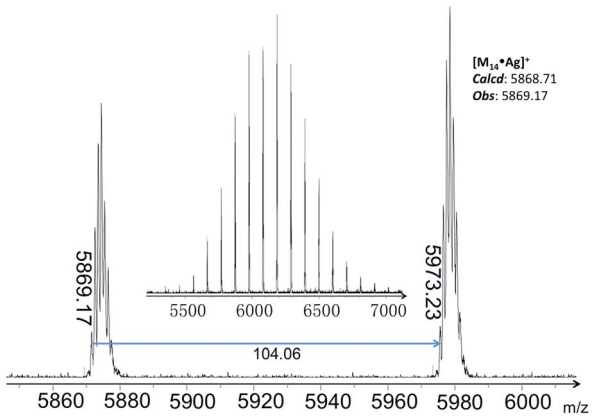

Fig. 5 MALDI-TOF mass spectrum of FPOSS-PS. The results are based on the sample FPOSS-PS_{24}.

$[C_{211}H_{190}F_{119}N_3O_{18}S_7Si_8Ag]^+$). The difference between two neighboring peaks is 104.06 Da, corresponding to the mass of one styrene repeating unit. All these molecular characterizations clearly confirm the success of this model reaction. The detailed molecular characterization data are summarized in Table 1.

3.3 Tethering multiple FPOSS units onto a polystyrene chain

Attaching multiple fluorous clusters is a convenient way to tune the fluorous content. Increasing the fluoro content in materials is especially critical to enhance the surface properties. In this section, we try to demonstrate the installation of multiple FPOSS nanoparticles onto a single polymer chain. The synthetic route is illustrated in Scheme 4. To prepare PS with multiple reactive azido functionalities along the polymer chain, 4-vinyl benzyl chloride is co-polymerized with styrene using RAFT polymerization, followed by nucleophilic substitution with sodium azide.[42] The FPOSS is then installed *via* the CuAAC "click" reaction.

The RAFT polymerization was carried out using ETC as the chain transfer agent and AIBN as the initiator. The conversion was kept below 50% to maintain a narrow molecular weight distribution.[43] The overall molecular weight was controlled by the polymerization time while the average number of VBC repeating units per polymer chain was adjusted through the feed ratio of two monomers. This number can be determined based on the ^{1}H NMR results by the integration ratio between the resonance peaks corresponding to the protons on the methylene groups adjacent to the chloride (4.51 ppm, proton b in Fig. 6a) and the protons on the chain transfer agent (3.2–3.4 ppm, proton a) (eqn (S2), see ESI† for detailed calculation). The overall molecular weight is also calculated based on the PS standard calibration. A narrow distribution is observed in the SEC chromatogram with PDI = 1.03 (Fig. 7, red).

The chloro groups along the PS chain can be readily converted to azido functionality by treating with sodium azide in

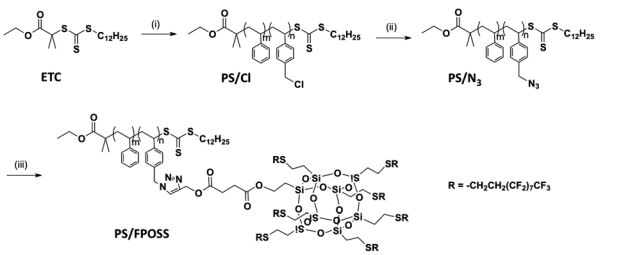

Scheme 4 Synthetic route towards PS/FPOSS: (i) AIBN, toluene, styrene, VBC, 110 °C, 41%; (ii) NaN_3, DMF, r.t., 80%; (iii) CuBr, PMDETA, TFT, 24h, r.t., 71%.

Table 1 Molecular characterization of FPOSS-containing polymers

Label	M_n[a] (kg mol^{-1})	M_n^{PEO}[b] (kg mol^{-1})	M_n^{PS}[c] (kg mol^{-1})	N_{FPOSS}[d]	PDI[e]	w_{FPOSS}[f] (%)
FPOSS-PS_{17}	5.8	—	1.7	0.95	1.11	70.6
FPOSS-PS_{24}	6.5	—	2.4	0.93	1.12	63.1
PS_{230}/$FPOSS_{10}$	64.0	—	23.0	9.3	1.12	64.1
FPOSS-PS_{28}-*b*-PEO_{45}	8.9	2.0	2.8	1.02	1.11	46.1
FPOSS-PS_{45}-*b*-PEO_{113}	13.6	5.0	4.5	0.92	1.08	30.1
PS_{38}-FPOSS-PEO_{45}	9.9	2.0	3.8	0.89	1.10	41.4
PS_{52}-FPOSS-PEO_{45}	11.3	2.0	5.2	1.05	1.08	36.3

[a] Overall molecular weight. [b] Molecular weight of PEO, calculated based on ^{1}H NMR. [c] Molecular weight of PS, calculated based on ^{1}H NMR. [d] Number of FPOSS per polymer chain, calculated based on ^{1}H NMR (see eqn (S1–S3) in the ESI). [e] Molecular weight distribution measured by SEC. [f] Weight percentage of FPOSS.

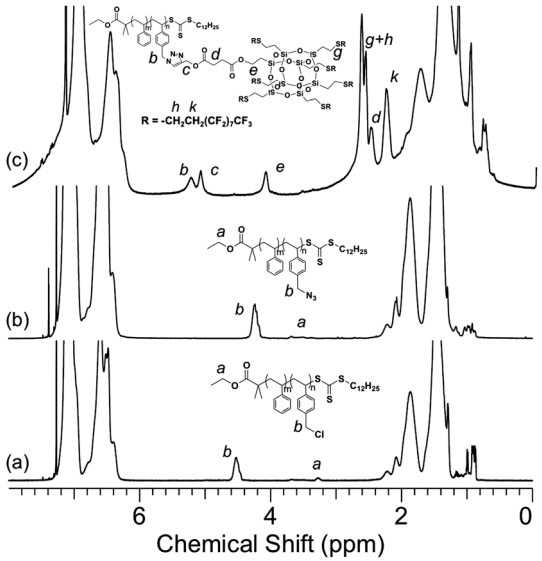

Fig. 6 ^{1}H NMR spectra of PS/Cl (a), PS/N_3 (b), and PS/FPOSS (c). The results are based on the sample PS_{230}/$FPOSS_{10}$.

DMF. Typical azide absorption is found in the FT-IR spectrum at 2100 cm^{-1} with a relatively strong intensity due to multiple azides per chain (Fig. S2 in the ESI†).[42] The ^{1}H NMR spectrum shows a complete resonance shift from δ 4.5 ppm to δ 4.3 ppm (proton b), indicating that all the chloro groups have been converted to the azido groups (Fig. 6b).

FPOSS can be readily attached onto PS/N_3 *via* "click" chemistry with high efficiency under mild conditions. In this case, excess FPOSS-alkyne is added to ensure that all the azide groups are consumed. No residual adsorption peak at 2100 cm^{-1} in the FT-IR spectrum was observed after the reaction (Fig. S2 in the ESI†). The SEC chromatograph shifts to a much lower retention volume, indicating an increase of the hydrodynamic volume due to incorporation of multiple FPOSSs (Fig. 7, blue). In the ^{1}H NMR spectrum, resonance from the FPOSS moiety can be clearly identified (Fig. 6c). The broad chemical shifts at δ 2.7 ppm (protons g and h) and δ 2.3 ppm (proton k) are assigned to the protons on the methylene adjacent to the sulfur and $-CF_2-$ group, respectively. The solubility of the product in common solvents is greatly enhanced. They can now be reversibly dissolved in most common organic solvents such as toluene, THF, $CHCl_3$, CH_2Cl_2, and others, even after long-term storage. The detailed molecular characterization data are also summarized in Table 1.

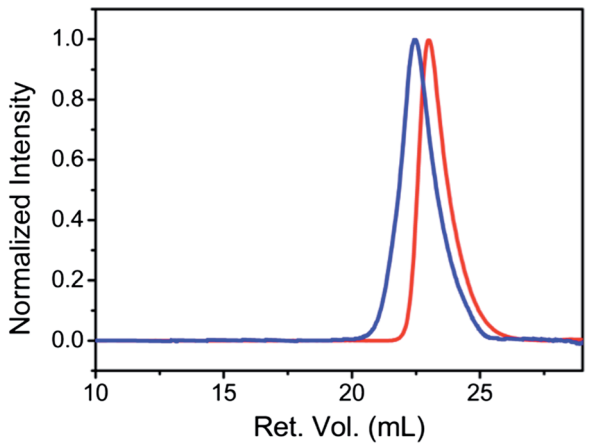

Fig. 7 SEC chromatograms of PS/Cl (red) and PS/FPOSS (blue). The results are based on the sample PS_{230}/$FPOSS_{10}$.

3.4 Giant surfactants based on FPOSS and the diblock copolymer

Thermodynamically stable phase morphologies, including lamellae (Lam), bicontinuous double gyroids (DG), hexagonal packed cylinders (Hex), and body-centred cubic packed spheres (BCC), together with several metastable phases, have been observed in diblock copolymers with chemically distinct

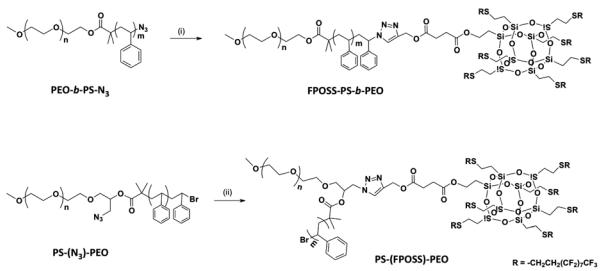

Scheme 5 Synthetic route towards giant surfactants based on FPOSS and the PS-*b*-PEO diblock copolymer: (i) CuBr, PMDETA, TFT, r.t., 71%; (ii) CuBr, PMDETA, TFT, r.t., 75%.

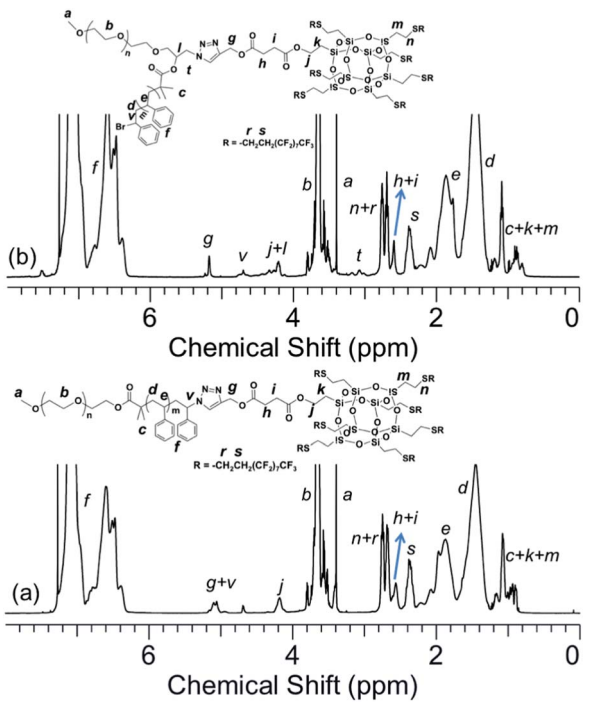

Fig. 8 ^{1}H NMR spectra of FPOSS-PS-*b*-PEO (a) and PS-(FPOSS)-PEO (b). The results are based on the sample FPOSS-PS_{28}-*b*-PEO_{45} and PS_{52}-(FPOSS)-PEO_{45}, respectively.

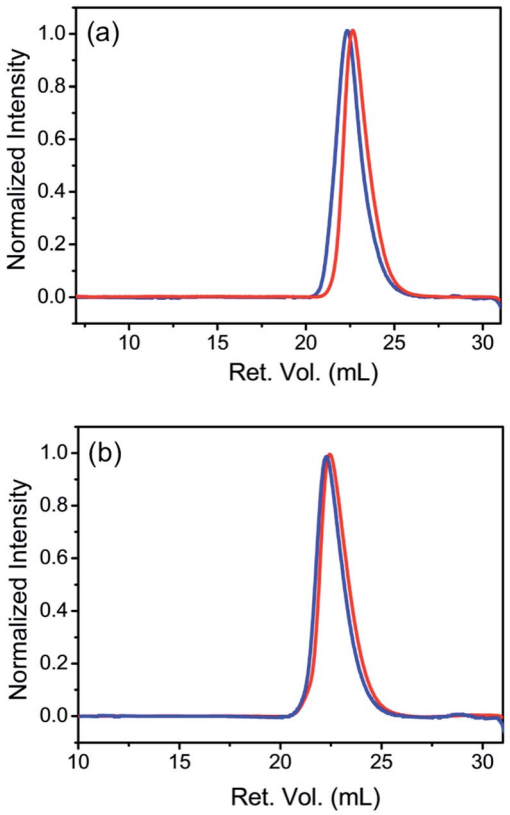

Fig. 9 SEC chromatograms of PEO-*b*-PS-N_3 (a, red), FPOSS-PS-*b*-PEO (a, blue), PS-(N_3)-PEO (b, red), and PS-(FPOSS)-PEO (b, blue). The results are based on the sample FPOSS-PS_{28}-*b*-PEO_{45} and PS_{52}-(FPOSS)-PEO_{45}, respectively.

components such as in the case of PS-*b*-PEO.[8,9,45–56] Providing an additional block will greatly expand the scope of assembled structures.[57] Incorporation of a "*third*" phase into amphiphilic diblock polymers will generate "triblock copolymer-like" giant surfactants with multiple interactions. This class of materials may expand the utility of block polymers and render them with novel self-assembly behaviors.[57] FPOSS could be an ideal candidate due to its precisely defined chemical structure and high immiscibility to both blocks.

Following a similar approach, we then extend our study to FPOSS-containing diblock copolymers. With proper design and synthesis of block polymer precursors with an azide functional group at a specific location, FPOSS can be precisely fixed at the chain end (FPOSS-PS-*b*-PEO), or at the junction point [PS-(FPOSS)-PEO] (Scheme 1). The synthetic route is outlined in Scheme 5.

As the first evidence of the success of this "click" reaction, the typical azide absorption bands at ~2100 cm^{-1} in the FT-IR spectra of both FPOSS-PS-*b*-PEO and PS-(FPOSS)-PEO disappear completely (Fig. S3 in the ESI†). In the ^1H NMR spectra, the signals corresponding to the FPOSS component at δ 2.7 ppm and δ 2.3 ppm can be clearly observed (Fig. 8a and b). A detailed assignment can be found in Fig. 8. The degree of functionality can be estimated based on the integrated peak area of the proton on the PEO block (δ 3.5–3.9 ppm, proton b) and the protons on the fluoroalkyl chains (δ 2.3–2.8 ppm, protons n, r, s, h, and i) (eqn (S3), see ESI† for detailed calculation). In both cases, the calculations indicate quantitative functionality. In the SEC chromatogram, a clear shift to a low retention volume can be found after the incorporation of FPOSS, due to the increase of the hydrodynamic volume (Fig. 9, blue). Both SEC chromatograms are narrow and symmetric, confirming the well-defined structures.

4 Conclusion

In summary, a "clickable" FPOSS with seven perfluorinated alkyl chains and one alkyne group, FPOSS-alkyne, has been synthesized and used as a versatile building block to introduce fluorous molecular clusters into other materials *via* CuAAC "click" chemistry. It provides an efficient and modular approach to construct FPOSS-containing polymers with various architectures and quantitative functionalities. FPOSS has been tethered onto PS or PS-*b*-PEO either at precise locations, including the chain end (FPOSS-PS, FPOSS-PS-*b*-PEO) and the junction point [PS-(FPOSS)-PEO], or randomly along the polymer chain (PS/FPOSS). Incorporation of the third fluorous phase will greatly expand the scope and utility of the shape amphiphiles. These precisely defined FPOSS-containing polymers can serve as model compounds to study their self assembly behaviors in the bulk, solution, and thin film.

Acknowledgements

This work was supported by the National Science Foundation (DMR-0906898 to S.Z.D.C.) and the Joint-Hope Education Foundation (to S.Z.D.C. and W.-B.Z.). The work in Sichuan University was also supported by a collaborative grant provided by the National Natural Science Foundation of China (51210005). We thank Ms Kai Guo and Prof. Chrys Wesdemiotis for their help with the MALDI-TOF mass characterization.

References

1 M. Cametti, B. Crousse, P. Metrangolo, R. Milani and G. Resnati, *Chem. Soc. Rev.*, 2012, **41**, 31–42.
2 J.-M. Vincent, *Chem. Commun.*, 2012, **48**, 11382–11391.
3 *Modern Fluoropolymers: High Performance Polymers for Diverse Applications*, ed. J. Scheirs, Wiley, Chichester, 1997.
4 *Handbook of Fluorous Chemistry*, ed. J. A. Gladysz, D. P. Curran and I. T. Horvath, Wiley-VCH, Weinheim, 2004.
5 J. A. Gladysz and M. Jurisch, *Structure, Physical and Chemical Properties of Fluorous Compounds*, Springer, Berlin, 2012.
6 A. Tuteja, W. Choi, J. M. Mabry, G. H. McKinley and R. E. Cohen, *Proc. Natl. Acad. Sci. U. S. A.*, 2008, **105**, 18200–18205.
7 E. d. Wolf, G. v. Koten and B.-J. Deelman, *Chem. Soc. Rev.*, 1999, **28**, 37–41.
8 F. S. Bates and G. H. Fredrickson, *Annu. Rev. Phys. Chem.*, 1990, **41**, 525–557.
9 F. S. Bates, *Science*, 1991, **251**, 898–905.

10 Z. Li, E. Kesselman, Y. Talmon, M. A. Hillmyer and T. P. Lodge, *Science*, 2004, **306**, 98–101.
11 S. Kubowicz, J. F. Baussard, J. F. Lutz, A. F. Thunemann, H. von Berlepsch and A. Laschewsky, *Angew. Chem., Int. Ed.*, 2005, **44**, 5262–5265.
12 J.-F. Lutz and A. Laschewsky, *Macromol. Chem. Phys.*, 2005, **206**, 813–817.
13 Z. Li, M. A. Hillmyer and T. P. Lodge, *Nano Lett.*, 2006, **6**, 1245–1249.
14 A. A. Gakh, A. A. Tuinman, J. L. Adcock, R. A. Sachleben and R. N. Compton, *J. Am. Chem. Soc.*, 1994, **116**, 819–820.
15 S. R. Wilson, V. Cayetano and M. Yurchenko, *Tetrahedron*, 2002, **58**, 4041–4047.
16 S. T. Iacono, A. Vij, W. Grabow, D. W. Smith and J. M. Mabry, *Chem. Commun.*, 2007, 4992–4994.
17 J. M. Mabry, A. Vij, S. T. Iacono and B. D. Viers, *Angew. Chem., Int. Ed.*, 2008, **47**, 4137–4140.
18 S. M. Ramirez, Y. J. Diaz, R. Campos, R. L. Stone, T. S. Haddad and J. M. Mabry, *J. Am. Chem. Soc.*, 2011, **133**, 20084–20087.
19 S. M. Ramirez, Y. J. Diaz, C. M. Sahagun, M. W. Duff, O. B. Lawal, S. T. Iacono and J. M. Mabry, *Polym. Chem.*, 2013, **4**, 2230–2234.
20 K. Zeng, L. Wang and S. Zheng, *J. Phys. Chem. B*, 2009, **113**, 11831–11840.
21 K. Zeng, L. Wang, S. Zheng and X. Qian, *Polymer*, 2009, **50**, 685–695.
22 L. Wang, K. Zeng and S. Zheng, *ACS Appl. Mater. Interfaces*, 2011, **3**, 898–909.
23 A. Tuteja, W. Choi, M. Ma, J. M. Mabry, S. A. Mazzella, G. C. Rutledge, G. H. McKinley and R. E. Cohen, *Science*, 2007, **318**, 1618–1622.
24 J. He, K. Yue, Y. Liu, X. Yu, P. Ni, K. A. Cavicchi, R. P. Quirk, E.-Q. Chen, S. Z. D. Cheng and W.-B. Zhang, *Polym. Chem.*, 2012, **3**, 2112–2120.
25 C. Hoyle and C. Bowman, *Angew. Chem., Int. Ed.*, 2010, **49**, 1540–1573.
26 A. B. Lowe, *Polym. Chem.*, 2010, **1**, 17–36.
27 X. Yu, S. Zhong, X. Li, Y. Tu, S. Yang, R. M. V. Horn, C. Ni, D. J. Pochan, R. P. Quirk, C. Wesdemiotis, W.-B. Zhang and S. Z. D. Cheng, *J. Am. Chem. Soc.*, 2010, **132**, 16741–16744.
28 W.-B. Zhang, Y. Li, X. Li, X. Dong, X. Yu, C.-L. Wang, C. Wesdemiotis, R. P. Quirk and S. Z. D. Cheng, *Macromolecules*, 2011, **44**, 2589–2596.
29 Y. Li, X.-H. Dong, K. Guo, Z. Wang, Z. Chen, C. Wesdemiotis, R. P. Quirk, W.-B. Zhang and S. Z. D. Cheng, *ACS Macro Lett.*, 2012, **1**, 834–839.
30 K. Yue, C. Liu, K. Guo, X. Yu, M. Huang, Y. Li, C. Wesdemiotis, S. Z. D. Cheng and W.-B. Zhang, *Macromolecules*, 2012, **45**, 8126–8134.
31 X.-H. Dong, R. Van Horn, Z. Chen, B. Ni, X. Yu, A. Wurm, C. Schick, B. Lotz, W.-B. Zhang and S. Z. D. Cheng, *J. Phys. Chem. Lett.*, 2013, **4**, 2356–2360.
32 H. Su, J. Zheng, Z. Wang, F. Lin, X. Feng, X.-H. Dong, M. L. Becker, S. Z. D. Cheng, W.-B. Zhang and Y. Li, *ACS Macro Lett.*, 2013, **2**, 645–650.
33 Z. Wang, Y. Li, X.-H. Dong, X. Yu, K. Guo, H. Su, K. Yue, C. Wesdemiotis, S. Z. D. Cheng and W.-B. Zhang, *Chem. Sci.*, 2013, **4**, 1345–1352.
34 X. Yu, K. Yue, I. F. Hsieh, Y. Li, X. H. Dong, C. Liu, Y. Xin, H. F. Wang, A. C. Shi, G. R. Newkome, R. M. Ho, E. Q. Chen, W. B. Zhang and S. Z. Cheng, *Proc. Natl. Acad. Sci. U. S. A.*, 2013, **110**, 10078–10083.
35 Y. Li, Z. Wang, J. Zheng, H. Su, F. Lin, K. Guo, X. Feng, C. Wesdemiotis, M. L. Becker, S. Z. D. Cheng and W.-B. Zhang, *ACS Macro Lett.*, 2013, **2**, 1026–1032.
36 Y. Li, K. Guo, H. Su, X. Li, Z. Wang, X. Feng, W. Zhang, S. Zhu, C. Wesdemiotis, S. Z. D. Cheng and W.-B. Zhang, *Chem. Sci.*, 2013, **4**, 1046–1053.
37 H. C. Kolb, M. G. Finn and K. B. Sharpless, *Angew. Chem., Int. Ed.*, 2001, **40**, 2004–2021.
38 V. V. Rostovtsev, L. G. Green, V. V. Fokin and K. B. Sharpless, *Angew. Chem., Int. Ed.*, 2002, **41**, 2596–2599.
39 F. J. Feher, K. D. Wyndham, R. K. Baldwin, D. Soulivong, J. D. Lichtenhan and J. W. Ziller, *Chem. Commun.*, 1999, 1289–1290.
40 C.-Y. Hong and C.-Y. Pan, *Macromolecules*, 2006, **39**, 3517–3524.
41 W.-B. Zhang, Y. Tu, R. Ranjan, R. M. V. Horn, S. Leng, J. Wang, M. J. Polce, C. Wesdemiotis, R. P. Quirk, G. R. Newkome and S. Z. D. Cheng, *Macromolecules*, 2008, **41**, 515–517.
42 X.-H. Dong, W.-B. Zhang, Y. Li, M. Huang, S. Zhang, R. P. Quirk and S. Z. D. Cheng, *Polym. Chem.*, 2012, **3**, 124–134.
43 D. J. Keddie, G. Moad, E. Rizzardo and S. H. Thang, *Macromolecules*, 2012, **45**, 5321–5342.
44 K. Matyjaszewski, *Macromolecules*, 2012, **45**, 4015–4039.
45 E. L. Thomas, D. B. Alward, D. J. Kinning, D. C. Martin, J. Dale, L. Handlin and L. J. Fetters, *Macromolecules*, 1986, **19**, 2197–2202.
46 K. Almdal, K. A. Koppi, F. S. Bates and K. Mortensen, *Macromolecules*, 1992, **25**, 1743–1751.
47 I. W. Hamley, K. A. Koppi, J. H. Rosedale and F. S. Bates, *Macromolecules*, 1993, **26**, 5959–5970.
48 D. A. Hajduk, P. E. Harper, S. M. Gruner, C. C. Honeker, G. Kim, E. L.Thomas and L. J. Fetters, *Macromolecules*, 1994, **27**, 4603–4705.
49 M. Schulz, F. Bates, K. Almdal and K. Mortensen, *Phys. Rev. Lett.*, 1994, **73**, 86–89.
50 L. Zhu, P. Huang, S. Z. D. Cheng, Q. Ge, R. Quirk, E. Thomas, B. Lotz, J.-C. Wittmann, B. Hsiao, F. Yeh and L. Liu, *Phys. Rev. Lett.*, 2001, **86**, 6030–6033.
51 R.-M. Ho, Y.-W. Chiang, C.-C. Tsai, C.-C. Lin, B.-T. Ko and B.-H. Huang, *J. Am. Chem. Soc.*, 2004, **126**, 2704–2705.
52 K. K. Tenneti, X. Chen, C. Y. Li, Y. Tu, X. Wan, Q.-F. Zhou, I. Sics and B. S. Hsiao, *J. Am. Chem. Soc.*, 2005, **127**, 15481–15490.
53 L. Zhu, S. Z. D. Cheng, B. H. Calhoun, Q. Ge, R. P. Quirk, E. L. Thomas, B. S. Hsiao, F. Yeh and B. Lotz, *Polymer*, 2001, **42**, 5829–5839.

54 L. Zhu, Y. Chen, A. Zhang, B. H. Calhoun, M. Chun, R. P. Quirk and S. Z. D. Cheng, *Phys. Rev. B: Condens. Matter Mater. Phys.*, 1999, **60**, 10022–10031.
55 L. Zhu, S. Z. D. Cheng, B. H. Calhoun, Q. Ge, R. P. Quirk, E. L. Thomas, B. S. Hsiao, F. Yeh and B. Lotz, *J. Am. Chem. Soc.*, 2000, **122**, 5957–5967.
56 L. Zhu, B. H. Calhoun, Q. Ge, R. P. Quirk, S. Z. D. Cheng, E. L. Thomas, B. S. Hsiao, F. Yeh, L. Liu and B. Lotz, *Macromolecules*, 2001, **34**, 1244–1251.
57 F. S. Bates, M. A. Hillmyer, T. P. Lodge, C. M. Bates, K. T. Delaney and G. H. Fredrickson, *Science*, 2012, **336**, 434–440.